Published OnlineFirst April 30, 2013; DOI: 10.1158/0008-5472.CAN-12-4579

Cancer Research

Conditional Loss of ErbB3 Delays Mammary Gland Hyperplasia Induced by Mutant *PIK3CA* without Affecting Mammary Tumor Latency, Gene Expression, or Signaling

Christian D. Young, Adam D. Pfefferle, Philip Owens, et al.

Cancer Res 2013;73:4075-4085. Published OnlineFirst April 30, 2013.

Published OnlineFirst April 30, 2013; DOI: 10.1158/0008-5472.CAN-12-4579

Therapeutics, Targets, and Chemical Biology

Cancer Research

Conditional Loss of ErbB3 Delays Mammary Gland Hyperplasia Induced by Mutant *PIK3CA* without Affecting Mammary Tumor Latency, Gene Expression, or Signaling

Christian D. Young[1], Adam D. Pfefferle[5,7], Philip Owens[2], María G. Kuba[3], Brent N. Rexer[1,4], Justin M. Balko[1], Violeta Sánchez[1], Hailing Cheng[8], Charles M. Perou[5,6,7], Jean J. Zhao[8], Rebecca S. Cook[2,4], and Carlos L. Arteaga[1,2,4]

Abstract

Mutations in *PIK3CA*, the gene encoding the p110α catalytic subunit of phosphoinositide 3-kinase (PI3K), have been shown to transform mammary epithelial cells (MEC). Studies suggest this transforming activity requires binding of mutant p110α via p85 to phosphorylated YXXM motifs in activated receptor tyrosine kinases (RTK) or adaptors. Using transgenic mice, we examined if ErbB3, a potent activator of PI3K, is required for mutant *PIK3CA*-mediated transformation of MECs. Conditional loss of ErbB3 in mammary epithelium resulted in a delay of $PIK3CA^{H1047R}$-dependent mammary gland hyperplasia, but tumor latency, gene expression, and PI3K signaling were unaffected. In ErbB3-deficient tumors, mutant PI3K remained associated with several tyrosyl phosphoproteins, potentially explaining the dispensability of ErbB3 for tumorigenicity and PI3K activity. Similarly, inhibition of ErbB RTKs with lapatinib did not affect PI3K signaling in $PIK3CA^{H1047R}$-expressing tumors. However, the p110α-specific inhibitor BYL719 in combination with lapatinib impaired mammary tumor growth and PI3K signaling more potently than BYL719 alone. Furthermore, coinhibition of p110α and ErbB3 potently suppressed proliferation and PI3K signaling in human breast cancer cells harboring $PIK3CA^{H1047R}$. These data suggest that $PIK3CA^{H1047R}$-driven tumor growth and PI3K signaling can occur independently of ErbB RTKs. However, simultaneous blockade of p110α and ErbB RTKs results in superior inhibition of PI3K and mammary tumor growth, suggesting a rational therapeutic combination against breast cancers harboring *PIK3CA* activating mutations. *Cancer Res; 73(13); 4075–85. ©2013 AACR.*

Introduction

Phosphoinositide 3-kinase (PI3K) is the most frequently mutated signaling pathway in cancer, affecting tumor cell survival, proliferation, migration, and metabolism (1, 2). PI3K is a lipid kinase composed of a p85 regulatory subunit dimerized with a p110 catalytic subunit (1, 3). The N-terminal SH2 domain of p85 binds to phosphorylated tyrosines in receptors or adaptors; this binding relieves the p85-mediated inhibition of p110 that, as a result, becomes activated and catalyzes the conversion of phosphatidylinositol-4,5-bisphosphate (PIP2) to phosphatidylinositol-3,4,5-trisphosphate (PIP3), a second messenger that recruits signal transducers (Akt, PDK1, SGK, etc.) to the plasma membrane, where they become activated (1).

The PI3K pathway is aberrantly activated by gain-of-function mutations in p110α (*PIK3CA*) and p85α (*PIK3R1*), amplification of wild-type *PIK3CA*, p110β (*PIK3CB*), and PDK1, loss/inactivation of the PIP3 phosphatases PTEN and INPP4B, mutation and/or amplification of AKT1-3, and amplification of receptor tyrosine kinases (RTK; refs. 4, 5). Three "hotspot" mutations have been identified in *PIK3CA*: E542K, E545K, and H1047R, accounting for approximately 80% of *PIK3CA* mutations (2, 6, 7). *PIK3CA* mutations occur in approximately 40% of breast cancers, mainly in tumors with luminal and HER2-enriched gene expression (8), where they have been associated with a more virulent phenotype and resistance to antiestrogen and anti-HER2 therapy.

HER2/ErbB2 gene amplification occurs in 25% of breast cancers where it associates with poor patient outcome. The main dimerization partner of HER2 is HER3/ErbB3. Six p85-binding motifs in ErbB3 activate PI3K (9, 10). ErbB3 is essential for PI3K activation and survival of HER2-overexpressing breast cancer cells (9, 11, 12). Therapies that inhibit PI3K induce ErbB3 expression and reactivation via feedback mechanisms, which partially maintain PI3K and counteract drug action. As

Authors' Affiliations: Departments of [1]Medicine, [2]Cancer Biology, and [3]Pathology, Vanderbilt University; [4]Breast Cancer Research Program, Vanderbilt-Ingram Cancer Center, Nashville, Tennessee; Departments of [5]Pathology and Laboratory Medicine and [6]Genetics; [7]Lineberger Comprehensive Cancer Center, University of North Carolina, Chapel Hill, North Carolina; and [8]Department of Cancer Biology, Dana-Farber Cancer Institute, Boston, Massachusetts

Note: Supplementary data for this article are available at Cancer Research Online (http://cancerres.aacrjournals.org/).

R.S. Cook and C.L. Arteaga contributed equally to this work.

Corresponding Author: Carlos L. Arteaga, Div. Hematology-Oncology, Vanderbilt University Medical Center, 2220 Pierce Avenue, 777 PRB, Nashville, TN 37232. Phone: 615-936-3524; Fax: 615-936-1790; E-mail: carlos.arteaga@vanderbilt.edu

doi: 10.1158/0008-5472.CAN-12-4579

Published OnlineFirst April 30, 2013; DOI: 10.1158/0008-5472.CAN-12-4579

such, the efficacy of HER2 and PI3K inhibitors is improved by coinhibition of ErbB3 (11, 13, 14).

In addition to ErbB2/ErbB3, other RTKs activate PI3K via insulin receptor substrate (IRS) and Gab family molecules. These adaptors lack enzymatic activity, but when tyrosine phosphorylated by RTKs, they recruit p85 (PI3K) and other signaling molecules (15, 16). Activated RTKs, including insulin and insulin-like growth factor (IGF) receptors, VEGF receptor (VEGFR), EGF receptor (EGFR), and ALK recruit IRS adaptors (16, 17). IRS-1 has 9 p85-binding motifs (18) and, like ErbB3, strongly activates PI3K. Similarly, Gab1 and Gab2 contain 3 p85-binding motifs and are tyrosine phosphorylated by ErbB2, MET, Abl, FGFR, EGFR, and Src kinases (15). The p85 subunit was discovered by its association with platelet-derived growth factor receptor (PDGFR), a potent activator of PI3K (19). Biochemical analyses have shown that both PIK3CA^{E545K} and PIK3CA^{H1047R} exhibit approximately 2-fold higher catalytic activity than wild-type PI3K. The association of PIK3CA^{H1047R} with PDGFR or IRS-1 phosphopeptides further increases the catalytic activity of the mutant enzyme (20). In addition, PIK3CA^{H1047R} association with p85 is required for transformation induced by mutant PI3K (6, 21). These data suggest a role for upstream RTKs in the signaling output of mutant PI3K, leading us to hypothesize that mutant *PIK3CA* requires upstream adaptors, such as ErbB3, to induce epithelial transformation and tumor progression.

We show herein that mammary gland hyperplasia induced by temporally regulated expression of mutant *PIK3CA* was delayed in mice lacking ErbB3 in the mammary epithelium. In contrast, tumor formation and PI3K activity were unaffected by ErbB3 ablation. In tumors expressing ErbB3, mutant PI3K associated with several tyrosine-phosphorylated proteins, including ErbB3. In tumors lacking ErbB3, PI3K still associated with other upstream adaptors and RTKs. Inhibition of RTKs or adaptors known to activate PI3K did not block cell growth or PI3K activity in mammary tumors or *PIK3CA*-mutant human breast cancer cells. However, simultaneous inhibition of upstream RTKs and mutant p110α more potently inhibited tumor growth and PI3K signaling than inhibition of p110α alone. These data suggest that mutant *PIK3CA* still relies upon upstream activators and combined inhibition of PI3K and these activators is a rational treatment strategy against tumors harboring *PIK3CA*-activating mutations.

Materials and Methods

Cell culture

MDA-MB-453 and T47D cells were from American Type Culture Collection. MDA-MB-453 were authenticated in March 2013 by short tandem repeat DNA analysis (DDC Medical); authentication of T47D cells (March 2011) has been described previously (22). CAL-148 and BT20 cells were provided and authenticated as described previously (23). All cells were cultured in Dulbecco's Modified Eagle Medium (DMEM) with 10% FBS (Life Technologies). EZN-3920 and EZN-4455 are locked nucleic acid (LNA) antisense molecules provided by Enzon Pharmaceuticals (11, 24); they were resuspended in sterile PBS to a stock concentration of 5 mmol/L and applied to cells at 5 μmol/L in the absence of transfection reagent. EZN-3920 targets ErbB3 and EZN-4455 is a scrambled control antisense. BYL719 (25) and LJM716 (26), provided by Novartis, were resuspended to a stock concentration of 1 mmol/L in dimethyl sulfoxide (DMSO) or 10 mg/mL in sterile PBS, respectively. siRNA (Qiagen) were transfected at a final concentration of 50 nmol/L total siRNA using Lipofectamine RNAiMAX (Life Technologies) following the manufacturer's protocol (see Supplementary Methods). The duration and concentration of each drug or siRNA treatment is described with each figure. Media and inhibitors were replenished every 3 days. Colony growth was assessed by plating cells and staining with crystal violet as detailed in Supplementary Methods.

Mice

To generate the iPIK3.iCre.ErbB3$^{FL/FL}$ model on a congenic FVB background, the following FVB mouse strains were interbred: *MMTV-rtTA* (27), *Tet-Op-HA-PIK3CA^{H1047R}-IRES-Luc* (28), *Tet-Op-Cre* (29), and *ErbB3$^{FL/FL}$* (30) as described in Supplementary Methods. Details of tumor transplantation are also provided in Supplementary Methods. Briefly, harvested tumors were homogenized in serum-free media with gentleMACS C Tubes (Miltenyi Biotec) and resuspended in 7 mL Matrigel diluted with 50% PBS. Tumor homogenates (100 μL) were injected into both inguinal (#4) mammary fat pads of 4-week-old female athymic mice (Harlan Laboratories) using a 25-gauge needle. When tumors reached 125 mm^3, mice were randomized to 4 treatment groups as indicated in figure legends. Lapatinib di-p-toluenesulfonate salt and imatinib methanesulfonate salt were purchased from LC Laboratories. Lapatinib, imatinib, and BYL719 were resuspended in 0.5% methyl cellulose, 0.1% Tween-80 for treatment by orogastric gavage. Lapatinib and imatinib were administered twice daily at 100 mg/kg/dose and BYL719 once daily at 30 mg/kg/dose. In the first study, all mice were sacrificed when tumors in vehicle-treated mice exceeded 1.5 cm^3. In the second study, animals with tumors greater than 1.0 cm^3 were sacrificed and all remaining animals were sacrificed on day 21. Mice were always sacrificed 1 hour after drug treatment.

Protein and histologic analyses

Cell line and tumor protein lysates were prepared as described in Supplementary Methods. Immunoprecipitation was conducted with a p85 (Millipore) or a hemagglutinin (HA) antibody (Cell Signaling Technology) using a ratio of 1 μg antibody: 250 μg lysate: 5 μL Dynal protein G beads (Life Technologies) with end-over-end rotation at 4°C for 4 hours. For immunoblot analysis, equal amounts of protein/lane were subjected to SDS-PAGE, transferred to nitrocellulose membranes, and analyzed with antibodies as described in Supplementary Methods. Phospho-RTK arrays were purchased from R&D Systems and incubated with 225 μg cell lysates following manufacturer's directions. Details of guinea pig anti-cytokeratin 8 (RDI-Fitzgerald) and rabbit anti-cytokeratin 5 (Covance) immunofluorescent staining of tissue sections and hematoxylin staining of whole mount mammary glands are provided in Supplementary Methods.

Published OnlineFirst April 30, 2013; DOI: 10.1158/0008-5472.CAN-12-4579

Gene expression analyses

Tumor RNA was harvested from ErbB3$^{FL/+}$ and ErbB3$^{FL/FL}$ iPIK3.iCre tumors and analyzed by cDNA microarray as described previously (31, 32). Briefly, RNA isolated by Qiagen RNeasy mini kit was hybridized to Agilent custom 4 × 180 K microarrays as previously described (31); the signal from iPIK3.Cre RNA was normalized to the Herschkowitz and colleagues murine dataset (32). The mutant *PIK3CA* gene signature (33) was calculated for every genotype in the Herschkowitz and colleagues mouse tumor dataset (32) and the iPIK3.iCre tumors. The average gene signature scores for each tumor class were plotted as boxplots to compare mutant *PIK3CA*-induced gene expression across previously defined classes (32).

Statistical analyses

Significant differences ($P < 0.01$) were determined by ANOVA and Bonferroni *post hoc* tests (multiple testing-corrected) or Student *t* test using Graphpad Prism software.

Results

ErbB3 inhibition sensitizes mutant *PIK3CA* breast cancer cells to a p110α inhibitor

ErbB3 silencing impairs the proliferative advantage conferred by mutant *PIK3CA* in *HER2*-amplified breast cancer cells (34). However, the impact of ErbB3 in *PIK3CA*-mutant breast cells lacking *HER2* amplification is less clear. We treated, MDA-MB-453, T47D, BT20, and CAL-148 breast cancer cells, all harboring *PIK3CA*^{H1047R}, with the ErbB3-neutralizing antibody, LJM716 (26), and BYL719, a p110α-specific inhibitor with an IC_{50} against wild-type and mutant p110α of ≤5 nmol/L (25). BYL719 decreased the proliferation (Fig. 1A–D) and Akt phosphorylation (Fig. 1E–H) of all 4 cell lines in a dose-dependent fashion, suggesting p110α^{H1047R} is a driver of proliferation and PI3K activity in these cells. LJM716 reduced basal and BYL719-induced total and Y1289-P-ErbB3 (Fig. 1E–H) and enhanced BYL719-mediated growth inhibition in each cell line (Fig. 1A–D), albeit weakly in T47D and CAL-148 cells. We also used EZN-3920, a LNA ErbB3-targeted antisense or a scrambled control LNA antisense, EZN-4455 (11, 24), in combination with BYL719. EZN-3920 did not reduce ErbB3 expression in MDA-MB-453 or T47D cells (Fig. 1I). EZN-3920 reduced ErbB3 levels and BYL719-induced Y1289-P-ErbB3 in both BT20 and CAL-148 cells (Fig. 1L and M). The combination of BYL719+EZN-3920 exhibited a better antiproliferative effect than either agent alone (Fig. 1J and K). In addition, increased T308-P-Akt induced by EZN-3920 was abrogated by BYL719 (Fig. 1L and M). These data suggest that coinhibition of ErbB3 and p110α impairs the proliferative advantage conferred by mutant *PIK3CA* in breast cancer cells without HER2 gene amplification.

Loss of ErbB3 delays mammary gland hyperplasia induced by mutant *PIK3CA*, but does not delay tumor formation

To evaluate whether ErbB3 is required for *PIK3CA*^{H1047R}-induced mammary epithelial cell (MEC) transformation *in vivo*, we generated transgenic mice in which doxycycline-induced *PIK3CA*^{H1047R} drives mammary tumor formation in the presence or absence of ErbB3. These mice expressed 3 transgenes [*MMTV-rtTA* (27), *Tet-Op-HA-PIK3CA*^{H1047R}*-IRES-Luc* (28), and *Tet-Op-Cre* (29)] and harbored homozygous or heterozygous floxed *ERBB3* alleles (Supplementary Fig. S1; refs. 11, 30, 35). In this model, referred to as iPIK3.iCre, doxycycline treatment simultaneously induced the expression of hemagglutinin-tagged *PIK3CA*^{H1047R} and Cre recombinase in the mammary epithelium, resulting in Cre-mediated recombination of floxed *ERBB3* alleles in MECs expressing *PIK3CA*^{H1047R}. The internal ribosomal entry site (IRES)-*Luciferase* allows bioluminescent detection of cells/tissues expressing *PIK3CA*^{H1047R}.

The mammary ductal epithelium in 6-week-old ErbB3$^{FL/+}$ (control) animals extended distally past the central lymph node, whereas the epithelium of ErbB3$^{FL/FL}$ mice was maintained proximal to the lymph node (Supplementary Fig. S2A; ref. 36). At 9 weeks, the ErbB3$^{FL/FL}$ ductal epithelium extended past the lymph node, but remained shorter than that of ErbB3$^{FL/+}$ animals (Supplementary Fig. S2B). Mammary ductal hyperplasia (induced by mutant *PIK3CA*) was not apparent in either group at 6 or 9 weeks of age (Supplementary Fig. S2A and S2B). By 12 weeks, ErbB3$^{FL/+}$ glands exhibited thickened, irregular ductal epithelium indicative of hyperplasia. However, ErbB3$^{FL/FL}$ iPIK3.iCre glands contained smooth, normal-appearing ducts (Fig. 2A and Supplementary Fig. S2C). Quantitation of epithelial content in whole mounts showed that ErbB3$^{FL/+}$ glands contained 80% more epithelium than ErbB3$^{FL/FL}$ glands (Fig. 2A). Histologic examination of mammary gland sections from 12-week-old animals showed that the ErbB3$^{FL/+}$ iPIK3.iCre glands contained multiple cell layers of ductal epithelium, whereas the ErbB3$^{FL/FL}$ iPIK3.iCre epithelium was arranged in a single, smooth cell layer (Fig. 2B).

Mice were monitored for expression of *PIK3CA-IRES-Luciferase* by IVIS bioluminescence imaging (Supplementary Fig. S3). Tumor formation was monitored by mammary gland palpation through 600 days of age. Mice lacking the iPIK3 transgene or not induced with doxycycline failed to develop tumors or exhibit luciferase activity at any point. The mean mammary tumor latency was 398 days in ErbB3$^{FL/+}$ mice as compared with 419 days in ErbB3$^{FL/FL}$ mice ($P = 0.72$; Fig. 2C). Loss of ErbB3 did not affect the average number of tumors per animal: 1.75 tumors per ErbB3$^{FL/+}$ mouse and 1.55 tumors per ErbB3$^{FL/FL}$ mouse ($P = 0.71$). These data suggest that loss of ErbB3 delays early mammary hyperplasia but not cancer formation in *PIK3CA*^{H1047R}-expressing mice.

Loss of ErbB3 does not alter PI3K signaling, histology, or gene expression in tumors induced by mutant *PIK3CA*

Immunoblot analysis revealed loss of ErbB3 expression in ErbB3$^{FL/FL}$ tumors. All tumors expressed p110α and p85 subunits of PI3K as well as the hemagglutinin-tagged p110α^{H1047R} transgene. Levels of phosphorylated Akt, S6, and PDK1 were similar in ErbB3$^{FL/+}$ and ErbB3$^{FL/FL}$ tumors, suggesting loss of ErbB3 did not attenuate PI3K signaling in *PIK3CA*^{H1047R}-driven mammary tumors (Fig. 2D).

Global gene expression patterns in ErbB3-deficient and -competent tumors were assessed using cDNA microarrays.

Published OnlineFirst April 30, 2013; DOI: 10.1158/0008-5472.CAN-12-4579

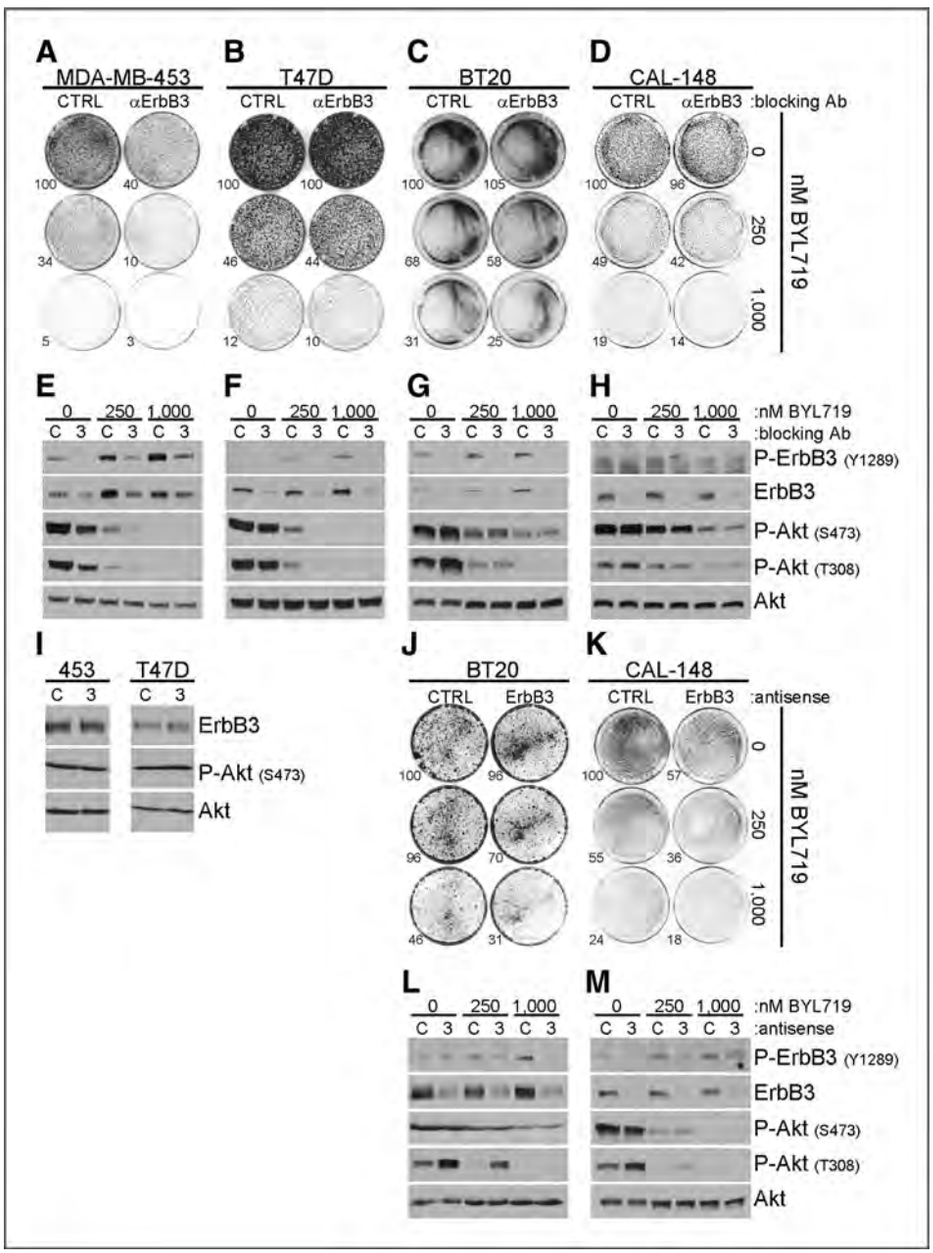

Figure 1. ErbB3 inhibition sensitizes mutant *PIK3CA* breast cancer cells to a p110α inhibitor. A–D, the indicated cell lines were treated with ±10 μg/mL LJM716, ErbB3-blocking antibody (Ab; αErbB3), and 0, 250, or 1,000 nmol/L BYL719 for 15 (MDA-MB-453 and T47D), 9 (BT20), or 12 days (CAL-148). Colonies were stained with crystal violet and quantitated using ImageJ software. Values shown are percentage growth relative to control-treated cells. E–H, cells were treated as described in A–D; after 4 days of treatment, cell lysates were prepared and subjected to immunoblot analysis with the indicated antibodies. I, MDA-MB-453 or T47D cells were treated 7 days with 5 μmol/L LNA antisense molecules without transfection reagent. EZN-4455, control LNA antisense (C), or EZN-3920, ErbB3-targeted LNA antisense (3), was used. Lysates were prepared and subjected to immunoblot analysis with the indicated antibodies. J and K, BT20 cells were treated 15 days or CAL-148 cells were treated 12 days with 5 μmol/L control LNA antisense (CTRL) or ErbB3-targeted LNA antisense (ErbB3) without transfection reagent and 0, 250, or 1,000 nmol/L BYL719. Growth was assessed as described in A–D. L and M, BT20 or CAL-148 cells were treated as described in J and K; after 7 days of treatment, cell lysates were prepared and subjected to immunoblot analysis with the indicated antibodies.

Unsupervised, hierarchical cluster analysis of iPIK3 tumors and 13 other genetically engineered mouse models (GEMM) of breast cancer (31, 32) showed ErbB3$^{FL/+}$ tumors did not segregate from ErbB3$^{FL/FL}$ tumors (Fig. 2E). Two-class significance analysis of microarray (SAM) analysis did not identify any differentially expressed genes in ErbB3$^{FL/+}$ and ErbB3$^{FL/FL}$ tumors. A previously reported mutant *PIK3CA* gene expression signature (33) showed that the *PIK3CA* signature was higher in the iPIK3.iCre models as compared with the other models (Fig. 2F), consistent with activation of the PI3K pathway. The

Published OnlineFirst April 30, 2013; DOI: 10.1158/0008-5472.CAN-12-4579

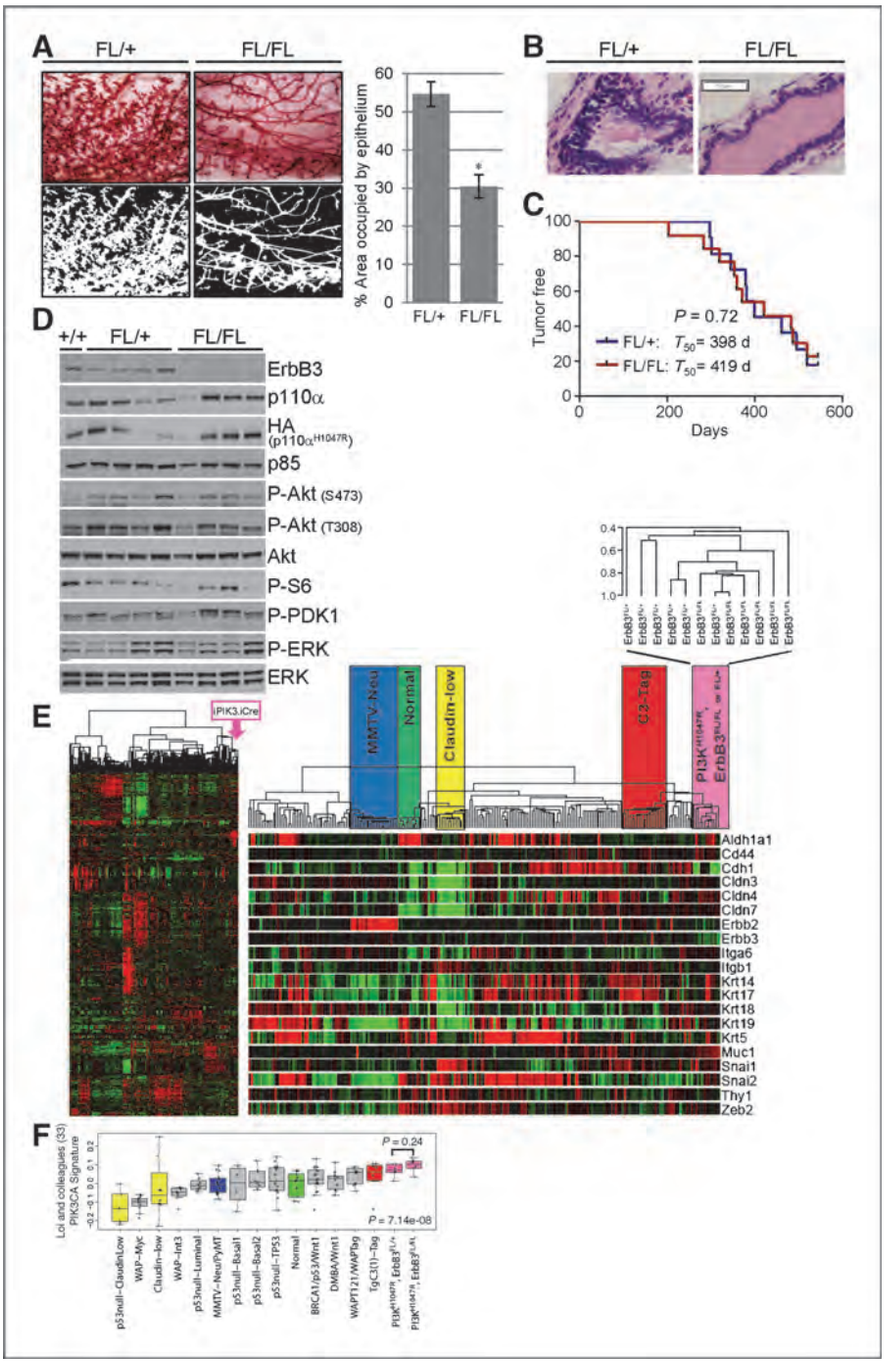

Figure 2. Loss of ErbB3 delays mammary gland hyperplasia induced by mutant *PIK3CA*, but does not delay tumor formation or alter PI3K signaling or gene expression. A, whole mount inguinal mammary glands from 12-week-old ErbB3$^{FL/+}$ and ErbB3$^{FL/FL}$ iPIK3.iCre mice were stained and photomicrographed at ×40 power (top) followed by conversion to binary pictures (bottom). The average percentage of area occupied by epithelium ±SEM was quantitated from 4 representative binary photomicrographs ($n = 3$ per genotype; right). *, $P < 0.01$. B, representative hematoxylin and eosin-stained sections of mammary glands harvested from 12-week-old ErbB3$^{FL/+}$ and ErbB3$^{FL/FL}$ iPIK3.iCre mice photomicrographed at ×400 power. C, Kaplan–Meier analysis of tumor-free survival of 11 ErbB3$^{FL/+}$ and 13 ErbB3$^{FL/FL}$ iPIK3.iCre mice. Average tumor latency = T_{50}. *P* value calculated using log-rank test. D, lysates were prepared from tumors harvested from 1 ErbB3$^{+/+}$, 4 ErbB3$^{FL/+}$, and 4 ErbB3$^{FL/FL}$ iPIK3.iCre mice and were subjected to immunoblot analysis with the indicated antibodies. E, left, unsupervised hierarchical cluster of 6 ErbB3$^{FL/+}$ and 6 ErbB3$^{FL/FL}$ iPIK3.iCre tumors with 13 previously characterized breast cancer GEMMs (32) using all probes with at least an absolute $\log_2$ expression value greater than 2 on at least 3 arrays (2,203 genes). Right, enlargement of the array dendrogram with common murine groups that represent human phenotypes highlighted for reference: MMTV-Neu (luminal), Normal breast, Claudin-low, and C3-Tag (basal-like). Beneath the dendrogram are 20 classic genes that segregate the intrinsic subtypes. The iPIK3.iCre dendrogram is enlarged to discern individual ErbB3$^{FL/+}$ and ErbB3$^{FL/FL}$ tumors. F, genes with a positive fold change in the mutant *PIK3CA* gene signature of Loi and colleagues (33) were averaged for each tumor in the combined murine dataset. These values were plotted by median expression for the defined murine classes (32) and the ErbB3$^{FL/+}$ and ErbB3$^{FL/FL}$ iPIK3.iCre tumors.

Published OnlineFirst April 30, 2013; DOI: 10.1158/0008-5472.CAN-12-4579

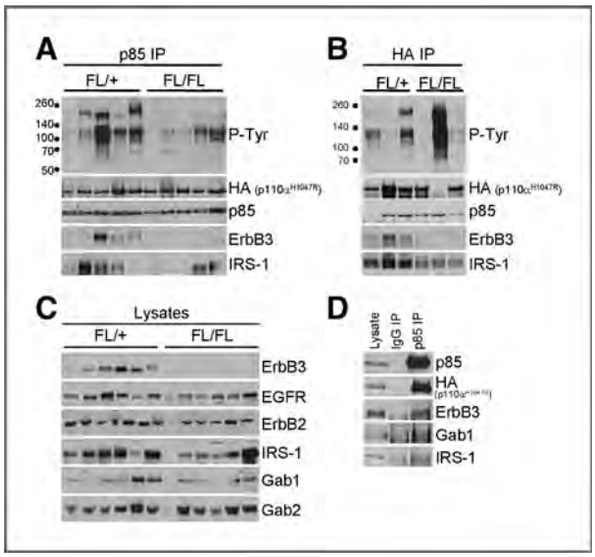

Figure 3. Mutant p110α binds to ErbB3 and other tyrosine-phosphorylated proteins. A, p85 was immunoprecipitated (IP) from 5 ErbB3$^{FL/+}$ and 5 ErbB3$^{FL/FL}$ primary tumor lysates. Immune complexes were prepared as indicated in Materials and Methods and subjected to immunoblot analysis with the indicated antibodies. B, hemagglutinin-tagged p110α^{H1047R} was immunoprecipitated from the lysates of 3 ErbB3$^{FL/+}$ and 3 ErbB3$^{FL/FL}$ tumors. Immune complexes were analyzed as described in A. C, lysates of 6 ErbB3$^{FL/+}$ and 6 ErbB3$^{FL/FL}$ iPIK3.iCre primary tumors were evaluated by immunoblot analysis with the indicated antibodies. D, an iPIK3.iCre tumor lysate was subjected to immunoprecipitation with control IgG or p85 antibodies. Whole lysates and antibody pull downs were evaluated by immunoblot analysis with the indicated antibodies.

mutant *PIK3CA* signature score was similar in ErbB3$^{FL/+}$ and ErbB3$^{FL/FL}$ tumors, suggesting loss of ErbB3 did not reduce PI3K signaling output.

Histologic examination of iPIK3 tumors revealed heterogeneous histopathologies (Supplementary Fig. S4A). The most frequent histologies were adenocarcinoma and adenocarcinoma with squamous metaplasia. Squamous metaplasia occurred more frequently in ErbB3$^{FL/FL}$ samples, whereas metaplastic carcinomas and adenomyoepithelioma-like lesions were unique to ErbB3$^{FL/+}$ tumors. ErbB3$^{FL/+}$ and ErbB3$^{FL/FL}$ tumors often displayed cribriform architecture, but tumors with papillary architecture occurred more frequently in ErbB3$^{FL/FL}$ mice and tumors with solid architecture were only seen in ErbB3$^{FL/+}$ mice (Supplementary Fig. S4B). *PIK3CA*-mutant mammary tumors have been reported to coexpress both luminal-type (i.e., CK8) and basal-type cytokeratins (i.e., CK5; refs. 37, 38). This was seen in ErbB3$^{FL/+}$ and ErbB3$^{FL/FL}$ cancers (Supplementary Fig. S4C). Thus, loss of ErbB3 did not enrich for either the luminal or basal population. These data are consistent with 2 recent reports (28, 38).

Mutant p110α binds to ErbB3 and other tyrosine-phosphorylated proteins

Because ErbB3 loss did not attenuate iPIK3.iCre tumorigenesis or PI3K signaling, we sought to determine if PIK3CA^{H1047R} engaged other tyrosine-phosphorylated adaptors or receptors. We detected hemagglutinin-tagged p110α^{H1047R} in p85 immunoprecipitates from ErbB3$^{FL/+}$ and ErbB3$^{FL/FL}$ tumor lysates (Fig. 3A, second and third rows). ErbB3 also coprecipitated with p85 in ErbB3$^{FL/+}$, but not ErbB3$^{FL/FL}$ tumors. Several tyrosine-phosphorylated proteins coprecipitated with p85 in ErbB3-deficient tumors (Fig. 3A). Immunoprecipitation of mutant p110α using an anti-hemagglutinin antibody pulled down p85 and several tyrosine-phosphorylated proteins in ErbB3$^{FL/+}$ and ErbB3$^{FL/FL}$ tumor lysates, including ErbB3 in the ErbB3$^{FL/+}$ tumors (Fig. 3B). p85 or hemagglutinin frequently coprecipitated IRS-1, a known PI3K scaffold (Fig. 3A and B). ErbB3$^{FL/FL}$ tumors lacked detectable ErbB3, but expressed EGFR, ErbB2, IRS-1, and Gab1/2 at levels similar to ErbB3$^{FL/+}$ tumors (Fig. 3C). Association of p85 with ErbB3, Gab1, and IRS-1 in iPIK3 tumor lysates (Fig. 3D) suggests that multiple adaptors can simultaneously engage mutant p110α, perhaps rendering ErbB3 dispensable for activity and plasma membrane localization of *PIK3CA*^{H1047R}.

Because the *PIK3CA*^{H1047R}-mutant human breast cancer cell line T47D requires mutant p110α for growth and Akt phosphorylation (Fig. 1B and F), we assessed the requirement for PI3K-activating adaptors. ErbB3 siRNA reduced coprecipitation of ErbB3 with p85, but Gab2 and IRS-1 continued to associate with p85 following ErbB3 depletion (Fig. 4A). Furthermore, P-Akt levels were sustained following ErbB3 depletion, consistent with maintenance of PI3K signaling. We combined siRNA-mediated knockdown of ErbB3, Gab2, and/or IRS-1. Despite significant reduction of all 3 PI3K adaptors,

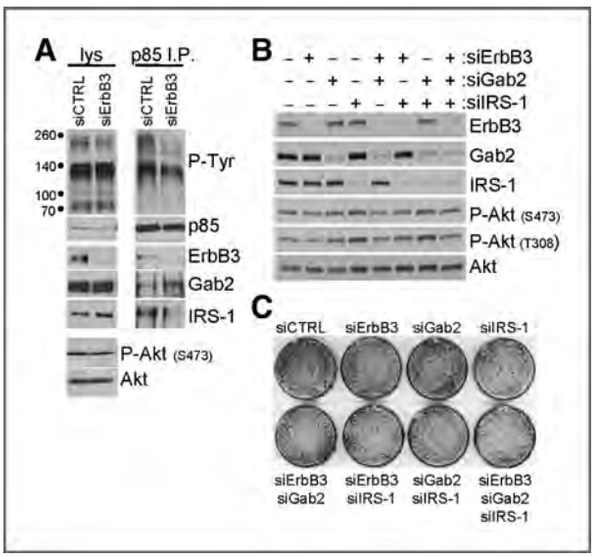

Figure 4. Loss of ErbB3, Gab2, and/or IRS-1 does not inhibit Akt or growth of T47D breast cancer cells. A, lysates (lys) or p85 immunoprecipitates (IP) from T47D cells transfected with control siRNA (siCTRL) or ErbB3 siRNA (siErbB3) collected 48 hours after transfection were evaluated by immunoblot analysis with the indicated antibodies. B, T47D cells were transfected with siRNA targeting ErbB3, Gab2, or IRS-1 as indicated with control siRNA being used such that 50 nmol/L total siRNA was always used. Lysates were prepared 48 hours after transfection and evaluated by immunoblot analysis with the indicated antibodies. C, T47D cells transfected with siRNA as described in B were stained with crystal violet 7 days after transfection.

Published OnlineFirst April 30, 2013; DOI: 10.1158/0008-5472.CAN-12-4579

Akt remained phosphorylated, suggesting that PI3K activity was not reduced (Fig. 4B). Similarly, proliferation was not dramatically altered by combined depletion of ErbB3, Gab2, and IRS-1 (Fig. 4C). These data suggest that because multiple proteins can engage mutant PI3K, depletion of ErbB3, Gab2, and/or IRS-1 is insufficient to reduce PI3K activity of tumors or cells driven by *PIK3CA*^{H1047R}.

ErbB RTK activity is dispensable in *PIK3CA*^{H1047R} tumors

To determine whether RTKs other than ErbB3 are activated in iPIK3.iCre tumors, we conducted phospho-RTK arrays. The most prominent tyrosine-phosphorylated RTKs in both ErbB3$^{FL/+}$ and ErbB3$^{FL/FL}$ tumors were ErbB2, EGFR, PDGFR, and macrophage-stimulating protein receptor (MSPR/Ron; Fig. 5A). One of the 8 tumors exhibited high P-HGFR, consistent with hepatocyte growth factor receptor (HGFR; *MET*) amplification previously reported in this model (28). We speculate the presence of these phosphorylated RTKs, all capable of engaging PI3K, may negate a requirement for ErbB3 in iPIK3 tumors.

To determine if inhibition of EGFR, ErbB2, and PDGFR would inhibit growth of *PIK3CA*^{H1047R}-expressing mammary tumors, we treated iPIK3.iCre tumor-bearing mice with (i) vehicle; (ii) EGFR/ErbB2 tyrosine kinase inhibitor (TKI) lapatinib; (iii) PDGFR TKI imatinib; and (iv) lapatinib + imatinib. Tumor growth was delayed by each single inhibitor and the combination (Fig. 5B). P-ErbB2 and P-EGFR levels were reduced by lapatinib, whereas imatinib inhibited P-PDGFRα and P-PDGFRβ (Fig. 5C). Imatinib-treated tumors exhibited higher levels of P-ErbB2 and P-EGFR, which were abolished in tumors cotreated with lapatinib. Although the combination of imatinib and lapatinib slowed tumor growth and inhibited ErbB/PDGFR phosphorylation, Akt and PDK1 remained phosphorylated in tumors treated with both RTK inhibitors (Fig. 5D). Pull down of p85 from tumor lysates coprecipitated IRS-1 and Gab1 as well as other tyrosine-phosphorylated proteins

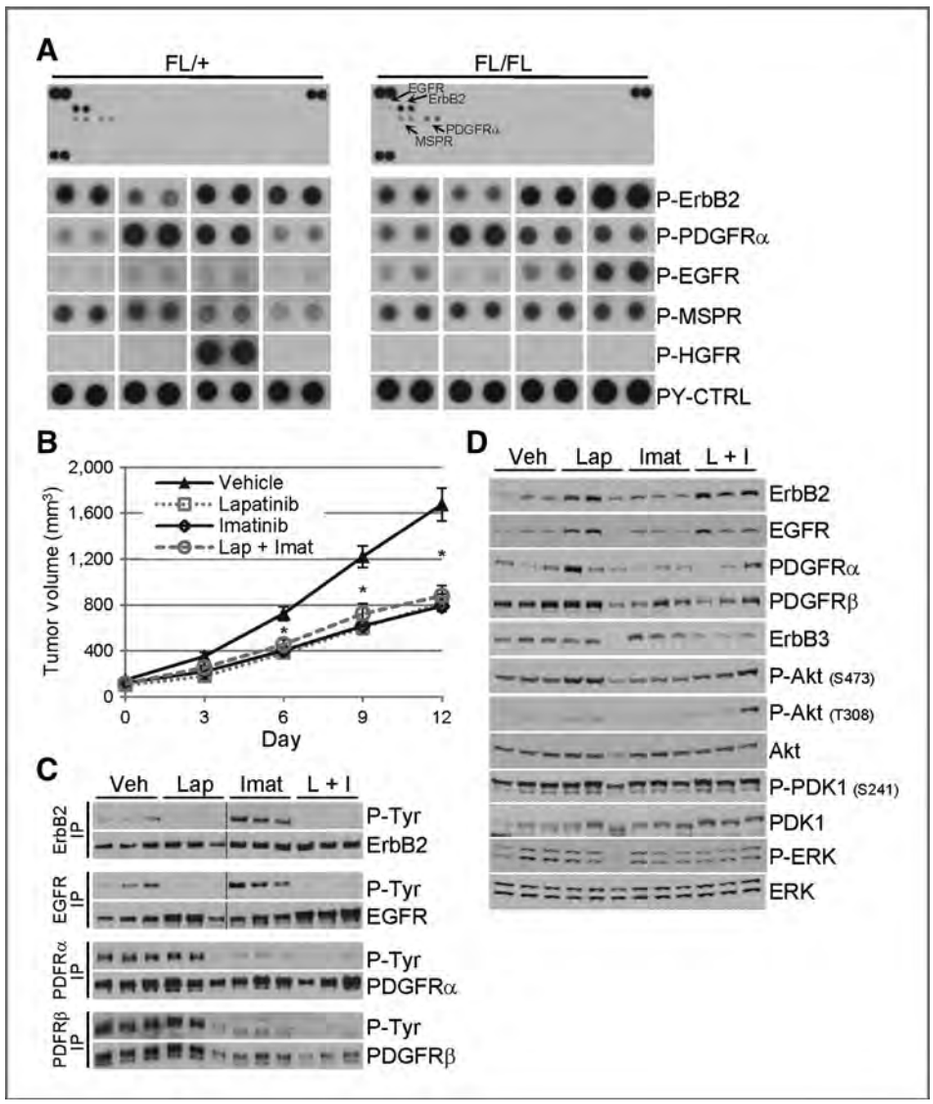

Figure 5. ErbB RTK activity is dispensable in *PIK3CA*^{H1047R} tumors. A, the lysates of 4 ErbB3$^{FL/+}$ and 4 ErbB3$^{FL/FL}$ primary tumors were applied to phospho-RTK arrays. One representative array of each genotype is presented (top) and enlarged, exposure-matched levels of ErbB2, PDGFRα, EGFR, MSPR, and HGFR are presented (bottom). B, mice bearing ≥125 mm^3 orthotopically transplanted iPIK3.iCre tumors were treated twice daily (100 mg/kg/dose) by orogastric gavage with vehicle (Veh), lapatinib (Lap), imatinib (Imat), or lapatinib + imatinib (L+I; 10 tumors/group). Average tumor volume for each group ±SEM is plotted against time. *, $P < 0.01$ (vehicle vs. treatment). C, three tumor lysates per group were subjected to immunoprecipitation (IP) with antibodies against ErbB2, EGFR, PDGFRα, or PDGFRβ. Antibody pull downs were subjected to immunoblot analysis with a P-Tyr antibody. Membranes were stripped and reprobed to detect the pulled down RTK. D, the same tumor lysates as in C were evaluated by immunoblot analysis with the indicated antibodies.

Published OnlineFirst April 30, 2013; DOI: 10.1158/0008-5472.CAN-12-4579

(Supplementary Fig. S5A and S5B). These data suggest that mutant PI3K engages multiple upstream adaptors, potentially explaining how it maintains its activity and effect on tumor growth despite inhibition of EGFR, ErbB2, and PDGFR kinases with a combination of small-molecule inhibitors.

Inhibition of *PIK3CA*^{H1047R}-driven tumor growth by a p110α inhibitor is enhanced by coinhibition of ErbB2/EGFR

Data shown in Figs. 2C–F, 4, and 5B–D suggest that targeted inhibition of signaling events upstream of PI3K, including ErbB3, EGFR, ErbB2, PDGFR, Gab2, or IRS-1, is insufficient to silence PI3K activity and tumor growth in *PIK3CA*^{H1047R}-driven cancers. Furthermore, compensatory upregulation of signaling networks upstream of PI3K can limit the therapeutic response to PI3K inhibitors (13, 39). To determine if this occurs in tumors that express *PIK3CA*^{H1047R} as the pathogenic oncogene, we treated iPIK3.iCre tumors with (i) vehicle; (ii) p110α-specific inhibitor BYL719; (iii) lapatinib; or (iv) lapatinib + BYL719. Although lapatinib slowed tumor growth less effectively than BYL719, the combination of lapatinib + BYL719 inhibited tumor growth more potently than either agent alone (Fig. 6A). Lapatinib reduced EGFR, ErbB2, and ErbB3 phosphorylation (Fig. 6B), but did not decrease P-PDK1 or P-Akt (Fig. 6C). BYL719 alone decreased P-Akt, but not P-PDK1. In contrast, BYL719 + lapatinib markedly reduced P-Akt and P-PDK1 levels (Fig. 6C), suggesting a more potent suppression of PI3K when p110α and EGFR/ErbB2/ErbB3 are inhibited simultaneously. BYL719 + lapatinib treatment slowed the weight gain of adolescent, tumor-bearing mice compared with mice treated with single agent BYL719 ($P < 0.01$), but histopathologic analysis revealed no liver damage in any treatment group (Supplementary Fig. S6).

To extend these observations, 4 human breast cancer cell lines with *PIK3CA*^{H1047R}, but without HER2 gene amplification (MDA-MB-453, T47D, BT20, and CAL-148), were treated with BYL719 and lapatinib. BYL719 reduced proliferation and P-Akt in all 4 cell lines (Fig. 7). Lapatinib inhibited basal and BYL719-induced phosphorylation of EGFR, ErbB2, and ErbB3 in each cell line (Fig. 7E–H). Lapatinib inhibited the proliferation of 2 cell lines as a single agent and aided the antiproliferative action of BYL719 in all 4 cell lines (Fig. 7A–D). Compared with single-agent treatments, the combination of BYL719 + lapatinib resulted in more potent inhibition of S473-P-Akt, T308-P-Akt, and P-S6 in MDA-MB-453 cells; S473-P-Akt, P-ERK, and P-S6 in T47D cells; P-PDK1 and P-ERK in BT20 cells; and T308-P-Akt, P-PDK1, and P-ERK in CAL-148 cells (Fig. 7E–H). Thus, while signaling downstream of PI3K was differentially affected by BYL719 and lapatinib in the 4 human cell lines and iPIK3.iCre transgenic mouse tumors, combined inhibition of p110α and ErbB receptors resulted in a more potent antitumor effect in all 5 *PIK3CA*^{H1047R}-driven models.

Discussion

PI3K is the most frequently mutated signaling pathway in breast cancer. Most common somatic alterations in this pathway are "hot spot" mutations in the helical and catalytic domains of *PIK3CA* (8). Transgenic mice with conditional expression of *PIK3CA*^{H1047R} in the mammary gland develop mammary cancers (28). Despite exhibiting a "gain-of-function,"

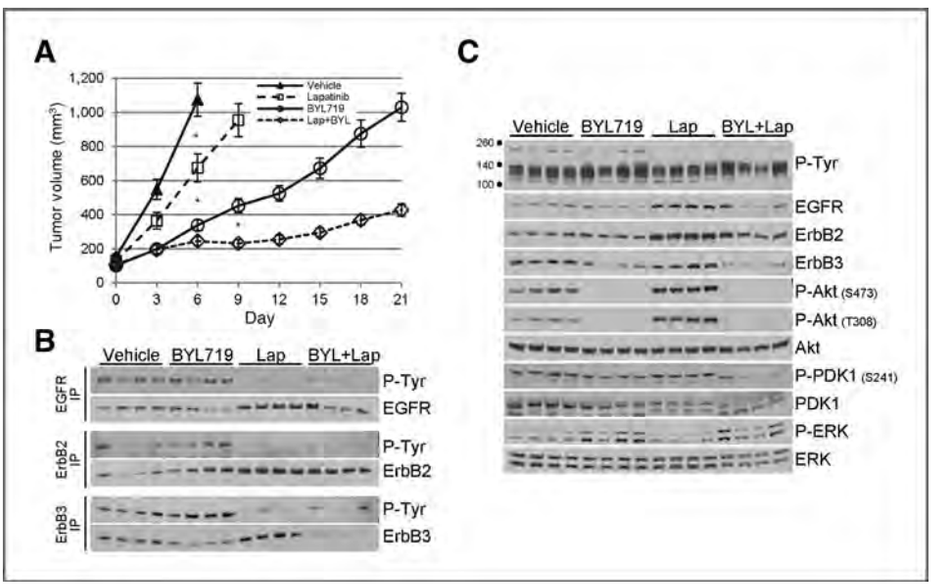

Figure 6. Growth of *PIK3CA*^{H1047R}-driven tumors is inhibited by combined blockade of p110α and ErbB2/EGFR. A, mice bearing ≥125 mm^3 orthotopically transplanted iPIK3.iCre tumors were treated with vehicle (twice daily), lapatinib (twice daily at 100 mg/kg/dose), BYL719 (once daily at 30 mg/kg/dose), or lapatinib + BYL719 (Lap+BYL; 14–16 tumors/group). Average tumor volume for each group ±SEM is plotted against time. *, $P < 0.01$ reported at earliest significant difference between groups. B, tumor lysates were subjected to immunoprecipitation (IP) with antibodies against EGFR, ErbB2, or ErbB3 and the resulting immune complexes evaluated by immunoblot analysis with a P-Tyr antibody. Membranes were stripped and re-probed to detect the pulled down RTK. C, the same tumor lysates as in B were evaluated by immunoblot analysis with the indicated antibodies.

Published OnlineFirst April 30, 2013; DOI: 10.1158/0008-5472.CAN-12-4579

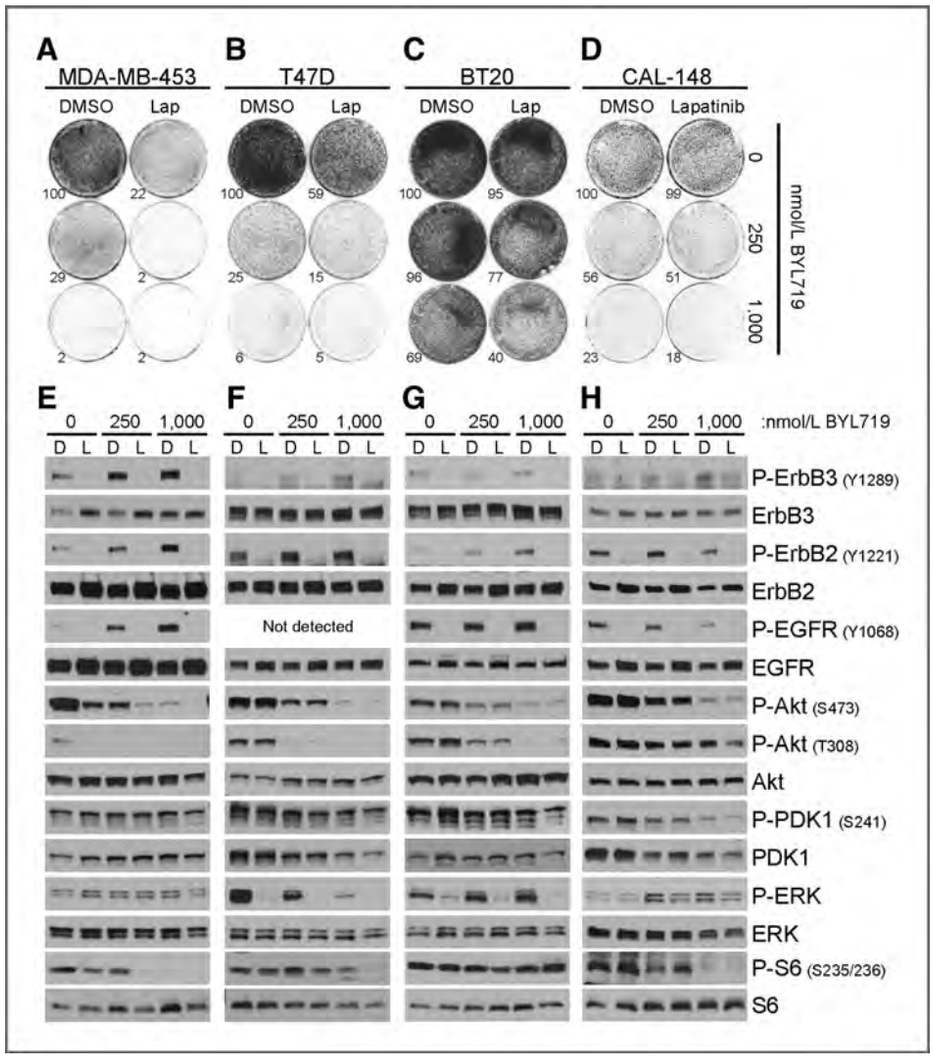

Figure 7. HER2 nonamplified human breast cancer cells with *PIK3CA*^{H1047R} are inhibited by combination of p110α inhibitor and lapatinib. A–D, the indicated cell lines were treated with DMSO or 500 nmol/L lapatinib (Lap) and 0, 250, or 1,000 nmol/L BYL719 for 10 days (MDA-MB-453), 14 days (T47D and BT20), or 12 days (CAL-148). Growth was assessed as described in Fig. 1. E–H, Cells were treated as described in A–D; after 3 days of treatment, cell lysates were prepared and subjected to immunoblot analysis with the indicated antibodies. (D, DMSO; L, lapatinib).

mutant *PIK3CA* still requires binding via the regulatory subunit p85 to phosphorylated adaptors or receptors. For example, *PIK3CA*^{H1047R}-mediated transformation of chick embryo fibroblast depends on its interaction with p85 (21) and the catalytic activity of PI3K^{H1047R} is enhanced by coupling to phosphorylated PDGFR or IRS-1 (20). Furthermore, knockdown of ErbB3 or its ligand heregulin inhibits growth and P-Akt levels in cells expressing *PIK3CA*^{H1047R} (34). Tissue-specific deletion of ErbB3 in the mammary gland results in a delay in ductal extension during puberty, increased apoptosis in terminal end buds (TEB) and a reduction in P-Akt (36), suggesting ErbB3-activated PI3K has an important role in mammary gland morphogenesis. Finally, Cre-mediated deletion of ErbB3 prolonged mammary tumor latency, reduced lung metastases and reduced P-Akt levels in mammary tumors driven by polyomavirus middle T oncogene (PyV mT; ref. 11). In this mouse model, PyV mT-driven tumor formation is highly dependent upon the association of middle T with p85 (40) and this association is lost upon deletion of ErbB3 or inhibition of ErbB3 phosphorylation with the EGFR/ErbB2 inhibitor lapatinib (11). These data suggest that ErbB3 is a major activator of wild-type and mutant PI3K in normal and transformed MECs. Thus, we examined if ErbB3 was required for MEC transformation by mutant PI3K.

We showed herein that loss of ErbB3 delayed mammary gland hyperplasia induced by mutant *PIK3CA*, but was dispensable for mammary tumorigenesis. This is in contrast to mammary tumors induced by the ErbB2/Neu transgene where loss of ErbB3 blocks mammary tumorigenesis (35). Our data are reminiscent of a recent study by Lahlou and colleagues, in which ErbB2/Neu-mediated hyperplasia, but not MEC transformation, was reduced by an ErbB3 mutant incapable of binding to p85 (PI3K; ref. 41). In tumors expressing the PI3K-uncoupled ErbB3 mutant, ErbB2 and EGFR engaged p85 to maintain PI3K activity. The iPIK3.iCre mice we present herein are phenotypically similar. It is unclear why genetic ablation of ErbB3 inhibits Neu-induced tumor formation (35), whereas uncoupling PI3K from ErbB3 does not (41), but the results suggest PI3K-independent functions of ErbB3.

Published OnlineFirst April 30, 2013; DOI: 10.1158/0008-5472.CAN-12-4579

Inhibition of EGFR/ErbB2 or PDGFR slowed mutant *PIK3CA* tumor growth without affecting Akt and PDK1 phosphorylation. This result suggests 2 not mutually exclusive possibilities. First, many RTKs or adaptors might contribute to PI3K activation in tumors harboring *PIK3CA* mutations. Second, the heightened activity of the $PIK3CA^{H1047R}$ kinase domain mutant (42, 43) allows for this kinase to signal strongly with fewer/no upstream binding partner(s). However, some upstream binding partners are likely needed because structural data suggest that p85 inhibits the catalytic activity of p110 until the p85/p110 complex binds to consensus phosphotyrosine YXXM motifs in RTKs/adaptors, thus relieving p85-mediated inhibition of p110 (44). E545K mutation in *PIK3CA* causes a structural change in the PI3K holoenzyme such that p85 no longer inhibits p110α, resulting in increased PI3K activity (45), which cannot be further activated by added tyrosine phosphorylated peptides (20). In contrast, the high kinase activity of H1047R PI3K doubles upon the addition of phospho-PDGFR or phospho-IRS-1 peptides (20). Finally, the transforming action of $PIK3CA^{H1047R}$, but not $PIK3CA^{E545K}$, is markedly reduced by loss of p85 binding, suggesting that $PIK3CA^{H1047R}$ requires binding to RTKs/adaptors for full activity (6, 21).

The driving oncogene in iPIK3.iCre tumors is $PIK3CA^{H1047R}$, making PI3K the most compelling therapeutic target. As a single agent, the p110α-specific inhibitor BYL719 reduced tumor growth and P-Akt in iPIK3.iCre tumors without effecting P-PDK1. Dual EGFR/ErbB2 and PI3K inhibition reduced P-Akt and P-PDK1 and decreased tumor growth better than either agent alone. These data suggest that while individual inhibition of mutant PI3K and RTKs upstream was insufficient to suppress PI3K activity and growth, ErbB inhibition significantly enhanced the effect of BYL719 against PI3K mutant cancers. This was recapitulated in $PIK3CA^{H1047R}$ human breast cancer cells. We speculate, however, that tumor cells not initially eliminated by combined ErbB and PI3K inhibition may allow mutant PI3K to engage other RTKs and adaptors, eventually allowing tumors to evade the antitumor effect of PI3K inhibitors.

Disclosure of Potential Conflicts of Interest

C.M. Perou is employed as a Board Member of University Genomics and BioClassifier LLC and has ownership interest (including patents) in University Genomics and Bioclassifier LLC. J.J. Zhao has other commercial research support from Novartis and is a consultant/advisory board member of the same. No potential conflicts of interest were disclosed by the other authors.

Authors' Contributions

Conception and design: C.D. Young, B.N. Rexer, C.L. Arteaga
Development of methodology: C.D. Young, B.N. Rexer, V. Sánchez, R.S. Cook
Acquisition of data (provided animals, acquired and managed patients, provided facilities, etc.): C.D. Young, A.D. Pfefferle, P. Owens, H. Cheng, J.J. Zhao, R.S. Cook
Analysis and interpretation of data (e.g., statistical analysis, biostatistics, computational analysis): C.D. Young, A.D. Pfefferle, P. Owens, M.G. Kuba, B.N. Rexer, J.M. Balko, C.M. Perou, C.L. Arteaga
Writing, review, and/or revision of the manuscript: C.D. Young, A.D. Pfefferle, C.M. Perou, R.S. Cook, C.L. Arteaga
Administrative, technical, or material support (i.e., reporting or organizing data, constructing databases): P. Owens, C.L. Arteaga
Study supervision: C.D. Young, C.L. Arteaga

Grant Support

This work was supported by R01 grants CA80195 (C.L. Arteaga) and CA143126 (R.S. Cook), American Cancer Society Clinical Research Professorship Grant CRP-07-234 (C.L. Arteaga), Breast Cancer Specialized Program of Research Excellence (SPORE) P50 CA98131, Vanderbilt-Ingram Cancer Center Support Grant P30 CA68485, a Stand Up to Cancer Dream Team Translational Research Grant from the Entertainment Industry Foundation (SU2C-AACR-DT0209), and Susan G. Komen for the Cure grants KG100677 (R.S. Cook), SAC100013 (C.L. Arteaga) and PDF12229712 (J.M. Balko). C.D. Young is supported by Department of Defense postdoctoral fellowship grant W81XWH-12-1-0026.

The costs of publication of this article were defrayed in part by the payment of page charges. This article must therefore be hereby marked *advertisement* in accordance with 18 U.S.C. Section 1734 solely to indicate this fact.

Received December 14, 2012; revised March 18, 2013; accepted April 5, 2013; published OnlineFirst April 30, 2013.

References

1. Engelman JA, Luo J, Cantley LC. The evolution of phosphatidylinositol 3-kinases as regulators of growth and metabolism. Nat Rev Genet 2006;7:606–19.
2. Bader AG, Kang S, Zhao L, Vogt PK. Oncogenic PI3K deregulates transcription and translation. Nat Rev Cancer 2005;5:921–9.
3. Yuan TL, Cantley LC. PI3K pathway alterations in cancer: variations on a theme. Oncogene 2008;27:5497–510.
4. Parsons R, Simpson L. PTEN and cancer. Methods Mol Biol 2003;222:147–66.
5. Courtney KD, Corcoran RB, Engelman JA. The PI3K pathway as drug target in human cancer. J Clin Oncol 2010;28:1075–83.
6. Zhao L, Vogt PK. Hot-spot mutations in p110alpha of phosphatidylinositol 3-kinase (pI3K): differential interactions with the regulatory subunit p85 and with RAS. Cell Cycle 2010;9:596–600.
7. Bader AG, Kang S, Vogt PK. Cancer-specific mutations in PIK3CA are oncogenic *in vivo*. Proc Natl Acad Sci U S A 2006;103:1475–9.
8. TCGA. Comprehensive molecular portraits of human breast tumours. Nature 2012;490:61–70.
9. Holbro T, Beerli RR, Maurer F, Koziczak M, Barbas CF III, Hynes NE. The ErbB2/ErbB3 heterodimer functions as an oncogenic unit: ErbB2 requires ErbB3 to drive breast tumor cell proliferation. Proc Natl Acad Sci U S A 2003;100:8933–8.
10. Schulze WX, Deng L, Mann M. Phosphotyrosine interactome of the ErbB-receptor kinase family. Mol Syst Biol 2005;1:2005.0008.
11. Cook RS, Garrett JT, Sanchez V, Stanford JC, Young C, Chakrabarty A, et al. ErbB3 ablation impairs PI3K/Akt-dependent mammary tumorigenesis. Cancer Res 2011;71:3941–51.
12. Junttila TT, Akita RW, Parsons K, Fields C, Lewis Phillips GD, Friedman LS, et al. Ligand-independent HER2/HER3/PI3K complex is disrupted by trastuzumab and is effectively inhibited by the PI3K inhibitor GDC-0941. Cancer Cell 2009;15:429–40.
13. Chakrabarty A, Sanchez V, Kuba MG, Rinehart C, Arteaga CL. Breast cancer special feature: feedback upregulation of HER3 (ErbB3) expression and activity attenuates antitumor effect of PI3K inhibitors. Proc Natl Acad Sci U S A 2012;109:2718–23.
14. Garrett JT, Olivares MG, Rinehart C, Granja-Ingram ND, Sanchez V, Chakrabarty A, et al. Transcriptional and posttranslational up-regulation of HER3 (ErbB3) compensates for inhibition of the HER2 tyrosine kinase. Proc Natl Acad Sci U S A 2011;108:5021–6.
15. Wohrle FU, Daly RJ, Brummer T. Function, regulation and pathological roles of the Gab/DOS docking proteins. Cell Commun Signal 2009;7:22.
16. Mardilovich K, Pankratz SL, Shaw LM. Expression and function of the insulin receptor substrate proteins in cancer. Cell Commun Signal 2009;7:14.

17. Myers MG Jr, Sun XJ, Cheatham B, Jachna BR, Glasheen EM, Backer JM, et al. IRS-1 is a common element in insulin and insulin-like growth factor-I signaling to the phosphatidylinositol 3′-kinase. Endocrinology 1993;132:1421–30.
18. Backer JM, Myers MG Jr, Shoelson SE, Chin DJ, Sun XJ, Miralpeix M, et al. Phosphatidylinositol 3′-kinase is activated by association with IRS-1 during insulin stimulation. EMBO J 1992;11:3469–79.
19. Escobedo JA, Navankasattusas S, Kavanaugh WM, Milfay D, Fried VA, Williams LT. cDNA cloning of a novel 85 kd protein that has SH2 domains and regulates binding of PI3-kinase to the PDGF beta-receptor. Cell 1991;65:75–82.
20. Carson JD, Van Aller G, Lehr R, Sinnamon RH, Kirkpatrick RB, Auger KR, et al. Effects of oncogenic p110alpha subunit mutations on the lipid kinase activity of phosphoinositide 3-kinase. Biochem J 2008;409:519–24.
21. Zhao L, Vogt PK. Helical domain and kinase domain mutations in p110alpha of phosphatidylinositol 3-kinase induce gain of function by different mechanisms. Proc Natl Acad Sci U S A 2008;105:2652–7.
22. Miller TW, Balko JM, Fox EM, Ghazoui Z, Dunbier A, Anderson H, et al. ERalpha-dependent E2F transcription can mediate resistance to estrogen deprivation in human breast cancer. Cancer Discov 2011;1:338–51.
23. Lehmann BD, Bauer JA, Chen X, Sanders ME, Chakravarthy AB, Shyr Y, et al. Identification of human triple-negative breast cancer subtypes and preclinical models for selection of targeted therapies. J Clin Invest 2011;121:2750–67.
24. Zhang Y, Qu Z, Kim S, Shi V, Liao B, Kraft P, et al. Down-modulation of cancer targets using locked nucleic acid (LNA)-based antisense oligonucleotides without transfection. Gene Ther 2011;18:326–33.
25. Huang A, Fritsch C, Wilson C, Reddy A, Liu M, Lehar J, et al. Single agent activity of PIK3CA inhibitor BYL719 in a broad cancer cell line panel [abstract]. In: Proceedings of the 103rd Annual Meeting of the American Association for Cancer Research; 2012 Mar 31–Apr 4; Chicago, IL. Philadelphia (PA): AACR; 2012. Abstract nr 3749.
26. Garner A, Sheng Q, Bialucha U, Chen D, Chen Y, Das R, et al. LJM716: an anti-HER3 antibody that inhibits both HER2 and NRG driven tumor growth by trapping HER3 in the inactive conformation [abstract]. In: Proceedings of the 103rd Annual Meeting of the American Association for Cancer Research; 2012 Mar 31–Apr 4; Chicago, IL. Philadelphia (PA): AACR; 2012. Abstract nr 2733.
27. Gunther EJ, Belka GK, Wertheim GB, Wang J, Hartman JL, Boxer RB, et al. A novel doxycycline-inducible system for the transgenic analysis of mammary gland biology. FASEB J 2002;16:283–92.
28. Liu P, Cheng H, Santiago S, Raeder M, Zhang F, Isabella A, et al. Oncogenic PIK3CA-driven mammary tumors frequently recur via PI3K pathway-dependent and PI3K pathway-independent mechanisms. Nat Med 2011;17:1116–20.
29. Guo ZM, Xu K, Yue Y, Huang B, Deng XY, Zhong NQ, et al. Temporal control of Cre recombinase-mediated *in vitro* DNA recombination by Tet-on gene expression system. Acta Biochim Biophys Sin (Shanghai) 2005;37:133–8.
30. Qu S, Rinehart C, Wu HH, Wang SE, Carter B, Xin H, et al. Gene targeting of ErbB3 using a Cre-mediated unidirectional DNA inversion strategy. Genesis 2006;44:477–86.
31. Herschkowitz JI, Simin K, Weigman VJ, Mikaelian I, Usary J, Hu Z, et al. Identification of conserved gene expression features between murine mammary carcinoma models and human breast tumors. Genome Biol 2007;8:R76.
32. Herschkowitz JI, Zhao W, Zhang M, Usary J, Murrow G, Edwards D, et al. Comparative oncogenomics identifies breast tumors enriched in functional tumor-initiating cells. Proc Natl Acad Sci U S A. 2012;109:2778–83.
33. Loi S, Haibe-Kains B, Majjaj S, Lallemand F, Durbecq V, Larsimont D, et al. PIK3CA mutations associated with gene signature of low mTORC1 signaling and better outcomes in estrogen receptor-positive breast cancer. Proc Natl Acad Sci U S A 2010;107:10208–13.
34. Chakrabarty A, Rexer BN, Wang SE, Cook RS, Engelman JA, Arteaga CL. H1047R phosphatidylinositol 3-kinase mutant enhances HER2-mediated transformation by heregulin production and activation of HER3. Oncogene 2010;29:5193–203.
35. Vaught DB, Stanford JC, Young C, Hicks DJ, Wheeler F, Rinehart C, et al. HER3 is required for HER2-induced preneoplastic changes to the breast epithelium and tumor formation. Cancer Res 2012;72:2672–82.
36. Balko JM, Miller TW, Morrison MM, Hutchinson K, Young C, Rinehart C, et al. The receptor tyrosine kinase ErbB3 maintains the balance between luminal and basal breast epithelium. Proc Natl Acad Sci U S A 2012;109:221–6.
37. Tikoo A, Roh V, Montgomery KG, Ivetac I, Waring P, Pelzer R, et al. Physiological levels of Pik3ca(H1047R) mutation in the mouse mammary gland results in ductal hyperplasia and formation of ERalpha-positive tumors. PLoS ONE 2012;7:e36924.
38. Meyer DS, Brinkhaus H, Muller U, Muller M, Cardiff RD, Bentires-Alj M. Luminal expression of PIK3CA mutant H1047R in the mammary gland induces heterogeneous tumors. Cancer Res 2011;71:4344–51.
39. Chandarlapaty S, Sawai A, Scaltriti M, Rodrik-Outmezguine V, Grbovic-Huezo O, Serra V, et al. AKT inhibition relieves feedback suppression of receptor tyrosine kinase expression and activity. Cancer Cell 2011;19:58–71.
40. Webster MA, Hutchinson JN, Rauh MJ, Muthuswamy SK, Anton M, Tortorice CG, et al. Requirement for both Shc and phosphatidylinositol 3′ kinase signaling pathways in polyomavirus middle T-mediated mammary tumorigenesis. Mol Cell Biol 1998;18:2344–59.
41. Lahlou H, Muller T, Sanguin-Gendreau V, Birchmeier C, Muller WJ. Uncoupling of PI3K from ErbB3 impairs mammary gland development but does not impact on ErbB2-induced mammary tumorigenesis. Cancer Res 2012;72:3080–90.
42. Samuels Y, Wang Z, Bardelli A, Silliman N, Ptak J, Szabo S, et al. High frequency of mutations of the PIK3CA gene in human cancers. Science 2004;304:554.
43. Isakoff SJ, Engelman JA, Irie HY, Luo J, Brachmann SM, Pearline RV, et al. Breast cancer-associated PIK3CA mutations are oncogenic in mammary epithelial cells. Cancer Res 2005;65:10992–1000.
44. Yu J, Zhang Y, McIlroy J, Rordorf-Nikolic T, Orr GA, Backer JM. Regulation of the p85/p110 phosphatidylinositol 3′-kinase: stabilization and inhibition of the p110alpha catalytic subunit by the p85 regulatory subunit. Mol Cell Biol 1998;18:1379–87.
45. Miled N, Yan Y, Hon WC, Perisic O, Zvelebil M, Inbar Y, et al. Mechanism of two classes of cancer mutations in the phosphoinositide 3-kinase catalytic subunit. Science 2007;317:239–42.